This paper is published as part of a PCCP Themed Issue on:
Coarse-grained modeling of soft condensed matter

Guest Editor: Roland Faller (UC Davis)

Editorial

Coarse-grained modeling of soft condensed matter
Phys. Chem. Chem. Phys., 2009 **DOI:** 10.1039/b903229c

Perspective

Multiscale modeling of emergent materials: biological and soft matter
Teemu Murtola, Alex Bunker, Ilpo Vattulainen, Markus Deserno and Mikko Karttunen, *Phys. Chem. Chem. Phys.*, 2009 **DOI:** 10.1039/b818051b

Communication

Dissipative particle dynamics simulation of quaternary bolaamphiphiles: multi-colour tiling in hexagonal columnar phases
Martin A. Bates and Martin Walker, *Phys. Chem. Chem. Phys.*, 2009 **DOI:** 10.1039/b818926a

Papers

Effective control of the transport coefficients of a coarse-grained liquid and polymer models using the dissipative particle dynamics and Lowe–Andersen equations of motion
Hu-Jun Qian, Chee Chin Liew and Florian Müller-Plathe, *Phys. Chem. Chem. Phys.*, 2009
DOI: 10.1039/b817584e

Adsorption of peptides (A3, Flg, Pd2, Pd4) on gold and palladium surfaces by a coarse-grained Monte Carlo simulation
R. B. Pandey, Hendrik Heinz, Jie Feng, Barry L. Farmer, Joseph M. Slocik, Lawrence F. Drummy and Rajesh R. Naik, *Phys. Chem. Chem. Phys.*, 2009 **DOI:** 10.1039/b816187a

A coarse-graining procedure for polymer melts applied to 1,4-polybutadiene
T. Strauch, L. Yelash and W. Paul, *Phys. Chem. Chem. Phys.*, 2009 **DOI:** 10.1039/b818271j

Anomalous waterlike behavior in spherically-symmetric water models optimized with the relative entropy
Aviel Chaimovich and M. Scott Shell, *Phys. Chem. Chem. Phys.*, 2009 **DOI:** 10.1039/b818512c

Coarse-graining dipolar interactions in simple fluids and polymer solutions: Monte Carlo studies of the phase behavior
B. M. Mognetti, P. Virnau, L. Yelash, W. Paul, K. Binder, M. Müller and L. G. MacDowell, *Phys. Chem. Chem. Phys.*, 2009 **DOI:** 10.1039/b818020m

Beyond amphiphiles: coarse-grained simulations of star-polyphile liquid crystalline assemblies
Jacob Judas Kain Kirkensgaard and Stephen Hyde, *Phys. Chem. Chem. Phys.*, 2009 **DOI:** 10.1039/b818032f

Salt exclusion in charged porous media: a coarse-graining strategy in the case of montmorillonite clays
Marie Jardat, Jean-François Dufrêche, Virginie Marry, Benjamin Rotenberg and Pierre Turq, *Phys. Chem. Chem. Phys.*, 2009 **DOI:** 10.1039/b818055e

Improved simulations of lattice peptide adsorption
Adam D. Swetnam and Michael P. Allen, *Phys. Chem. Chem. Phys.*, 2009 **DOI:** 10.1039/b818067a

Curvature effects on lipid packing and dynamics in liposomes revealed by coarse grained molecular dynamics simulations
H. Jelger Risselada and Siewert J. Marrink, *Phys. Chem. Chem. Phys.*, 2009 **DOI:** 10.1039/b818782g

Self-assembling dipeptides: conformational sampling in solvent-free coarse-grained simulation
Alessandra Villa, Christine Peter and Nico F. A. van der Vegt, *Phys. Chem. Chem. Phys.*, 2009 **DOI:** 10.1039/b818144f

Self-assembling dipeptides: including solvent degrees of freedom in a coarse-grained model
Alessandra Villa, Nico F. A. van der Vegt and Christine Peter, *Phys. Chem. Chem. Phys.*, 2009 **DOI:** 10.1039/b818146m

Computing free energies of interfaces in self-assembling systems
Marcus Müller, Kostas Ch. Daoulas and Yuki Norizoe, *Phys. Chem. Chem. Phys.*, 2009 **DOI:** 10.1039/b818111j

Anomalous ductility in thermoset/thermoplastic polymer alloys
Debashish Mukherji and Cameron F. Abrams, *Phys. Chem. Chem. Phys.*, 2009 **DOI:** 10.1039/b818039c

A coarse-grained simulation study of mesophase formation in a series of rod–coil multiblock copolymers
Juho S. Lintuvuori and Mark R. Wilson, *Phys. Chem. Chem. Phys.*, 2009 **DOI:** 10.1039/b818616b

Simulations of rigid bodies in an angle-axis framework
Dwaipayan Chakrabarti and David J. Wales, *Phys. Chem. Chem. Phys.*, 2009 **DOI:** 10.1039/b818054g

Effective force coarse-graining
Yanting Wang, W. G. Noid, Pu Liu and Gregory A. Voth, *Phys. Chem. Chem. Phys.*, 2009 **DOI:** 10.1039/b819182d

Backmapping coarse-grained polymer models under sheared nonequilibrium conditions
Xiaoyu Chen, Paola Carbone, Giuseppe Santangelo, Andrea Di Matteo, Giuseppe Milano and Florian Müller-Plathe, *Phys. Chem. Chem. Phys.*, 2009 **DOI:** 10.1039/b817895j

Energy landscapes for shells assembled from pentagonal and hexagonal pyramids
Szilard N. Fejer, Tim R. James, Javier Hernández-Rojas and David J. Wales, *Phys. Chem. Chem. Phys.*, 2009
DOI: 10.1039/b818062h

Molecular structure and phase behaviour of hairy-rod polymers
David L. Cheung and Alessandro Troisi, *Phys. Chem. Chem. Phys.*, 2009 **DOI:** 10.1039/b818428c

Molecular dynamics study of the effect of cholesterol on the properties of lipid monolayers at low surface tensions
Cameron Laing, Svetlana Baoukina and D. Peter Tieleman, *Phys. Chem. Chem. Phys.*, 2009 **DOI:** 10.1039/b819767a

On using a too large integration time step in molecular dynamics simulations of coarse-grained molecular models
Moritz Winger, Daniel Trzesniak, Riccardo Baron and Wilfred F. van Gunsteren, *Phys. Chem. Chem. Phys.*, 2009 **DOI:** 10.1039/b818713d

The influence of polymer architecture on the assembly of poly(ethylene oxide) grafted C_{60} fullerene clusters in aqueous solution: a molecular dynamics simulation study
Justin B. Hooper, Dmitry Bedrov and Grant D. Smith, *Phys. Chem. Chem. Phys.*, 2009 **DOI:** 10.1039/b818971d

Determination of pair-wise inter-residue interaction forces from folding pathways and their implementation in coarse-grained folding prediction
Sefer Baday, Burak Erman and Yaman Arkun, *Phys. Chem. Chem. Phys.*, 2009 **DOI:** 10.1039/b820801h

Beyond amphiphiles: coarse-grained simulations of star-polyphile liquid crystalline assemblies†

Jacob Judas Kain Kirkensgaard*[a] and Stephen Hyde*[b]

Received 14th October 2008, Accepted 18th December 2008
First published as an Advance Article on the web 28th January 2009
DOI: 10.1039/b818032f

We have simulated the self-assembly of a novel class of three-arm molecules, *ABC* star-architecture *polyphiles*, using coarse-grained bead simulations. A number of topologically complex liquid crystalline mesostructures arise that can be related to the better-known bicontinuous mesophases of lyotropic amphiphilic systems. The simulations reveal 3D self-assemblies whose structural variations follow those expected assuming a simple steric molecular packing model as a function of star polyphile splay and relative volumes of each arm in the polyphile. The splay of each arm, characterised by the 3D wedge-shape emanating from the core of each molecule to its exterior induces torsion of the interfaces along the triple lines, whereas differences in the relative volumes of arms induce curvature of the triple lines. Three distinct mesostructures are described, characterised by their micro-domain topologies, which are unknown in simpler amphiphilic systems, but resemble in some respects bicontinuous mesophases. These three- (or more) arm polyphilic systems offer an interesting extension to the better-known self-assembly of (two-arm) amphiphiles in solution.

I. Introduction

The mutual immiscibility of hydrophobic and hydrophilic domains within amphiphiles leads to a variety of supra-molecular mesostructures in solution, from micelles of various forms to folded bilayers. The shapes of these aggregates can be rationalised in terms of the preferred packing configurations of constituent molecules within the assemblies.[1] The binary character of amphiphiles leads to a natural description of amphiphilic mesostructures in terms of the two-dimensional interface that forms the common boundary between hydrophobic and hydrophilic domains; we describe the mesostructure in terms of the interfacial geometry. The approach extends naturally to a description of amphiphilic bilayers in terms of the bilayer curvatures.[2]

The generalisation to molecules with three or more mutually immiscible moieties, driving the spontaneous self-assembly of bulk molecular mixtures (possibly in solution) to form multiple domain types, has received relatively little attention. A notable exception is in the field of synthetic copolymer self-assembly, where the self-assembly of melts of so-called 'mikto-arm' copolymers has been explored experimentally and theoretically. These star-shaped molecules contain 3 or more arms, all covalently linked at one end *via* a common junction. The star architecture imposes additional topological constraints on supra-molecular assemblies; in particular, the associated mesostructures are characterised by the presence of one-dimensional multi-phase lines that describe the loci of the star junctions as well as two-dimensional interfaces, that separate all moiety pairs. For example, three-arm (*ABC*) mikto copolymer mesostructures are described by three-dimensional domains of *A*, *B* and *C* types, two-dimensional walls common to domains *AB*, *BC* and *CA* and one-dimensional *ABC* lines that bound all three domain types. The simplest structure that is consistent with the star topology of each molecule is a three-colored hexagonal honeycomb pattern, with adjacent cells bearing distinct colours, arranged such that each junction line is common to all three colours (see Fig. 3 below).

A number of experimental studies of three- and four-arm mikto copolymer melts have confirmed the formation of discrete domains, separated by two-phase walls and three- or four-phase lines.[3–14] To date, all reported mesostructures are (somewhat idealised) prismatic arrays made of extended rod-shaped domains, separated by planar interfaces, with molecular junctions lying on extended, uncurved three- or four-fold branch lines. Dotera and colleagues have developed a lattice model to simulate the self-assembly of three-arm copolymer melts and have largely confirmed these experimental findings. Their simulations have in addition revealed the possibility of a plethora of as yet unobserved mesostructures, formed by extending various tilings of the flat plane into the third dimension under pure translation normal to the plane (just as the hexagonal honeycomb is related to the hexagonal tiling of the plane). These planar tilings include most Archimedean tilings,[15–17] as well as quasi-crystalline patterns.[18] More recently, Huang *et al.* have implemented particle dynamics techniques to explore mikto-arm self-assembly as a function of the interactions between the molecular species making up the star copolymers.[19] Evidently, this is a rich field to explore further at both experimental and theoretical levels.

[a] *Dept. of Basic Sciences and Environment, Faculty of Life Sciences, Copenhagen University, Copenhagen, Denmark. E-mail: kirkensgaard@life.ku.dk*
[b] *Applied Mathematics, Research School of Physical Sciences, Australian National University, Canberra, Australia. E-mail: stephen.hyde@anu.edu.au*

† Electronic supplementary information (ESI) available: Simulation movies. See DOI: 10.1039/b818032f

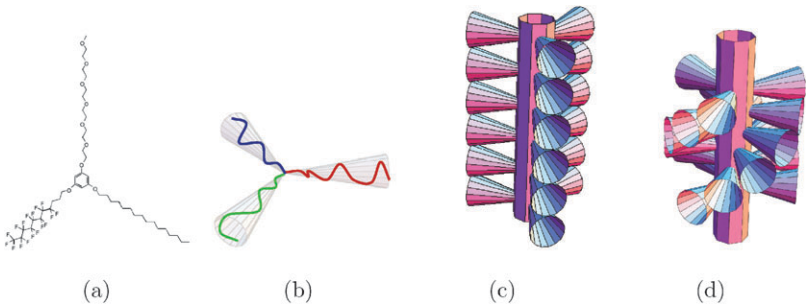

Fig. 1 (a) An example of a three-arm polyphile, with polyethylene glycol, fluorocarbon and hydrocarbon oligomeric chains linked to a common aromatic core, whose self-assembly in the presence of partially miscible solvents (water, hydrocarbon and fluorocarbon oils) is currently being studied. (b–d) Schematic cartoon of three-arm polyphile stacking along triple-lines. (b) Each arm is represented by a splayed (cone-shaped) block (with empty space between arms for clarity) and a single polyphile is the Y-shaped triplet of arms. (c) Adjacent polyphiles are stacked along the triple-line without twist. (d) Adjacent molecules are twisted along the axis of the triple-line, forcing the interfaces between pairs of arms to adopt a helicoidal form. Twisting allows the molecules to pack with reduced triple-line length, reducing the line tension (at the possible expense of increased surface tension in the interfaces).

We have commenced theoretical and experimental studies of self-assembly of multi-arm intermediate molecular-weight *oligomers* (rather than polymers) containing hydrophilic, oleophilic and fluorophilic moieties. We call such molecules (with more than two mutually immiscible moieties) *star polyphiles*. These molecules resemble amphiphiles, in that they can self-assemble in solution, with an additional fluorocarbon moiety that is designed to be essentially immiscible with the other two moieties. A number of star polyphiles are currently being studied. The most promising cases are all derived from the phloroglucinol molecule, with three arms covalently linked to the central aromatic core *via* oxygen atoms at the 2,4,6 positions on the ring. Those arms are an aliphatic hydrocarbon chain containing between twelve and twenty carbon atoms, a perfluorinated unbranched chain with seven or eight carbon atoms and a hydrophilic polyethylene glycol chain made of seven or eight monomers (see Fig. 1(a)). Scattering experiments and polarised optical microscopy confirm the possibility of self-assembly of three-arm star polyphiles into liquid crystalline mesophases.

A theory of self-assembly of star polyphiles is under development that builds on the notion of molecular packings, introduced for amphiphilic assemblies. This theory will be presented in detail elsewhere, here we offer only the essential skeleton that motivates our simulation studies reported below. The assembly is governed by the splay of each arm, just as amphiphilic mesostructure is set by the preferred splay of the hydrophobic chain ends. In order to achieve an optimal packing of splayed arms (and thereby minimise the length of the multi-phase lines per molecule), a relative twist between adjacent molecules may be expected, whose magnitude scales with the degree of splay of each arm (see Fig. 1). Thus, splay is related to line torsion in star polyphile assemblies. These packing considerations also lead to the possibility of curvature of the multi-phase lines, if the polyphile is 'unbalanced' with different volumes in distinct arms. To accommodate those differences, we may expect the lines to curve away from the bulkier arms. Note that the final structure must not only offer steric accommodation to the constituent polyphiles, it must also reduce the surface tension that depends on the interfacial area in the pattern. The resulting micro-domain pattern is one that manages to optimize the energetic trade-off that may arise between the requirements of steric packing, and minimal surface tension.

These heuristics lead us to expect a link between the star-polyphile geometry, manifested in the curvature and torsion of the multi-phase lines that thread the structure, *via* splay and relative volume of each constituent arm of the polyphile. These concepts—different to those of amphiphilic self-assembly—can nevertheless be thought of as natural extensions of the connection between amphiphilic membrane curvature and molecular shape.

We therefore expect to find star-polyphile structures (and, likely also mikto-arm copolymer assemblies) that exhibit generically curved and twisted multi-phase lines, beyond the straight lines of the prismatic cellular patterns described above, hitherto observed and modelled in copolymeric systems. This paper explores the validity of that claim in general terms, seeking evidence of line curvature and torsion in model star-polyphile assemblies.

II. Simulations

An elegantly simple coarse-grained approach to simulating self-assembly of amphiphilic mesoscale structures, particularly bilayer membrane systems, has been developed in the past few years.[20–23] The model has been demonstrated to reproduce key features of (lipid) amphiphile assemblies, most notably (for our purposes here) the formation of curved fluid bilayers, including the effect of constituent lipid shape on the resulting bilayer curvatures.[24] In contrast to most simulations of these systems, this approach ignores the presence of an explicit solvent. Instead, self-assembly is triggered by effective tail interactions between lipids, modelled as beads. Here we extend this model to explore the self-assembly of generic star polyphiles with mutually immiscible arms as a function of the splay and relative volumes of constituent arms.

Our model star-polyphiles are represented by beads as shown in Fig. 2. Each molecule consists of a neutral junction bead and an (in principle) arbitrary number of arms attached, in this case three. Each arm consists of two beads and has a separate 'color', meaning that it interacts differently with other

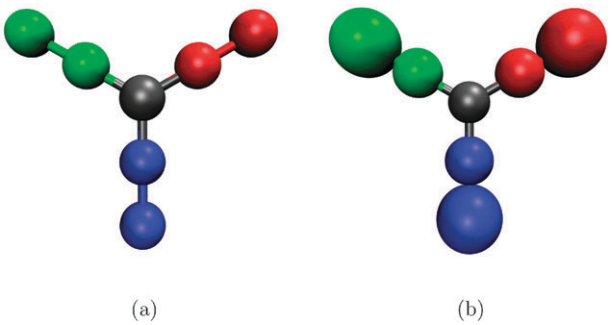

Fig. 2 (a) Rendering of the model star molecule. A neutral center junction connects 3 mutually immiscible arms, indicated by different colors. (b) A model star molecule with splayed arms.

beads according to their color. The self-assembly is initiated by effective attractions between like-coloured arms of different molecules. On the other hand, distinctly coloured arms repel, consistent with their mutual immiscibility. Imposition of strong repulsion between unlike-coloured arms is equivalent to the strong segregation limit of polymer theory.

A Simulation details

Molecular dynamics (MD) simulations are performed using a modified version of the mbtools extension to the Espresso package.[25] The full details of the original model can be found in ref. 20. Denoting our units of energy and length ε and σ respectively, all bead sizes are controlled *via* a repulsive truncated and shifted Lennard-Jones potential

$$V_{\mathrm{rep}}(r,b) = \begin{cases} 4\varepsilon\left[\left(\frac{b}{r}\right)^{12} - \left(\frac{b}{r}\right)^{6} + \frac{1}{4}\right] & \text{for } r \le r_c \\ 0 & \text{for } r > r_c \end{cases} \qquad (2.1)$$

with $r_c = 2^{1/6}b$. To simulate molecules with different arm volumes, we require beads of different sizes, so the magnitude of the bead diameter b is a variable parameter. Since b is defined through this pair-interaction, it is set to be the arithmetic mean of the diameters of the two interacting beads, *i.e.* invoking the Lorentz–Berthelot mixing rules. Connected beads along each arm are linked by a FENE bond

$$V_{\mathrm{bond}} = -\tfrac{1}{2}k_{\mathrm{bond}}r_{\infty}^2 \log[1 - (r/r_{\infty})^2] \qquad (2.2)$$

with stiffness $k_{\mathrm{bond}} = 30\varepsilon/\sigma^2$. The divergence length is usually set to $r_{\infty} = 1.5\sigma$, however, for large diameter beads this would result in a substantial potential overlap between neighboring beads of the same arm causing the simulations to crash. In these situations the value is set higher thus allowing the bond length to accommodate the relevant bead size. A harmonic spring acting between the junction bead and the last bead of each arm is used to straighten the arms,

$$V_{\mathrm{bend}} = -\tfrac{1}{2}k_{\mathrm{bend}}(r - 4\sigma)^2, \qquad (2.3)$$

where the bending stiffness $k_{\mathrm{bend}} = 10\varepsilon/\sigma^2$. The final interaction is the attraction which acts between all beads of same color (*i.e.* between like arms) according to

$$V_{\mathrm{attr}}(r,b) = \begin{cases} -\varepsilon & \text{for } r < r_c \\ -\varepsilon\cos^2\left[\frac{\pi(r-r_c)}{2w_c}\right] & \text{for } r_c \le r \le r_c + w_c \\ 0 & \text{for } r > r_c + w_c \end{cases} \qquad (2.4)$$

This is an attractive potential with potential depth ε and an interaction range set by w_c. Values of w_c around 1.2–1.6σ are found to be optimal in simulations of a pure 'balanced' star-polyphile, characterised by equal geometric characteristics of each arm and symmetric cross interactions within and between arms, which in this range self-assembles robustly to the hexagonal honeycomb at the employed temperature of $k_{\mathrm{B}}T = 1.5\varepsilon$. Under these conditions the system is far from the order–disorder transition (which does not occur unless $k_{\mathrm{B}}T > 3\varepsilon$ for the relevant values of w_c). In general we find that to achieve micro-domain segregation into 3 phases w_c must exceed 0.8 in agreement with ref. 20 for fluid bilayers. All simulations presented are with symmetric cross-interactions and $\sigma = 1$, $\varepsilon = 1$.

Simulations were performed as constant volume (NVT ensemble) simulations using a Langevin thermostat with time steps $\delta t = 0.01\tau$ and a friction constant $\Gamma = \tau^{-1}$ (in units of Lennard-Jones time τ). The simulated volume is a cubic box of side length L with period boundary conditions. All simulations are started from a random gas configuration and run until an equilibrium state is reached. This is usually easily determined visually, but is also monitored by looking at energy and pressure fluctuations. If no changes occur over a simulation period of several thousand time steps the system is considered to have reached equilibrium. Additional details of the different simulations are given below. Simulation movies available as ESI† were all made with the VMD package.[26]

III. Results

A Splay simulations

The splay of an arm is modeled simply by varying the diameter of the beads along the arm so as to approximate the shape of a cone (see Fig. 2). Denoting the diameter of the beads by d_i, where $i = 0,1,2$ for junction, first and second bead of each arm respectively, the diameters are calculated as

$$d_i = d_{i-1}\left(\frac{1 + \tan(\phi)}{1 - \tan(\phi)}\right), \qquad (3.5)$$

which follows from simple geometry. As mentioned earlier, b is set to be the arithmetic mean of whichever two bead diameters involved, *i.e.*

$$b_{ij} = \frac{d_i + d_j}{2}. \qquad (3.6)$$

So, a particular splay angle ϕ and junction bead diameter d_0 defines the other diameters and thus the b parameters needed for the simulations.

In Fig. 3 we see the result of simulating a geometrically balanced molecule (*i.e.* all arms are identical in length and volume) with no splay ($\phi = 0$). The system self-assembles to form the 3-colored hexagonal honeycomb, as expected. For low splay angles the hexagonal phase persists, but with increasing junction–junction distance along the multi-phase lines due to the increased volume of the splayed arms.

Increasing the splay angle to *ca.* $\phi = 10^{\circ}$ and higher, the system evolves into a novel three-dimensional 'tricontinuous' pattern, containing three mutually interwoven three-dimensional

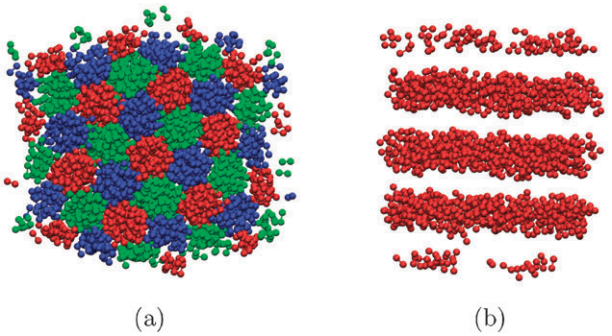

Fig. 3 Simulation snapshots of a 3-colored hexagonal honeycomb with red, blue and green arms, respectively. (a) Orthographic projection along a symmetry axis. (b) Orthographic projection perpendicular to a symmetry axis of the red phase alone showing the rod-like structure. Simulation details: 900 molecules, $L = 20\sigma$, $d_0 = 1\sigma$, $\phi = 0$, occupied volume fraction = 0.42, $k_BT = 1.5\varepsilon$, $w_c = 1.6\sigma$.

sponge-like domains, illustrated in Fig. 4. We have calculated the structure factors of each domain, determined from the Fourier transform of the bead positions. These are shown in Fig. 4. The structure factors of all three domains coincide, supporting our visual observation of congruent domains. However, we have not yet definitively identified the structure of this tricontinuous pattern.

We can, however, draw some conclusions from our own theoretical investigations of the geometrical features of tricontinuous patterns, consisting of three interwoven and geometrically identical labyrinths. A number of trisections of space into three equivalent, 3D domains have been constructed, and will be discussed in detail elsewhere. The variety of tricontinuous patterns is at least as rich as the plethora of bicontinuous forms that arise from the study of three-periodic minimal surfaces.[2] All tricontinuous patterns that we have constructed contain saddle-shaped hyperbolic branched interfaces, inducing non-zero torsion along these lines. Indeed, the tricontinuous structure detected by our simulations exhibits torsion along the triple lines, evidenced by the screw-like configuration of the interfaces in the vicinity of the triple lines. The triple lines found in these balanced cases also appears to be, on average, curvature-free.

B Simulating relative arm volumes

We can form 'unbalanced' polyphiles by changing the relative volumes of the arms, achieved by altering the diameter of the beads constituting distinct arms. Since the bond length is not completely fixed, the arm lengths shorten to varying degrees

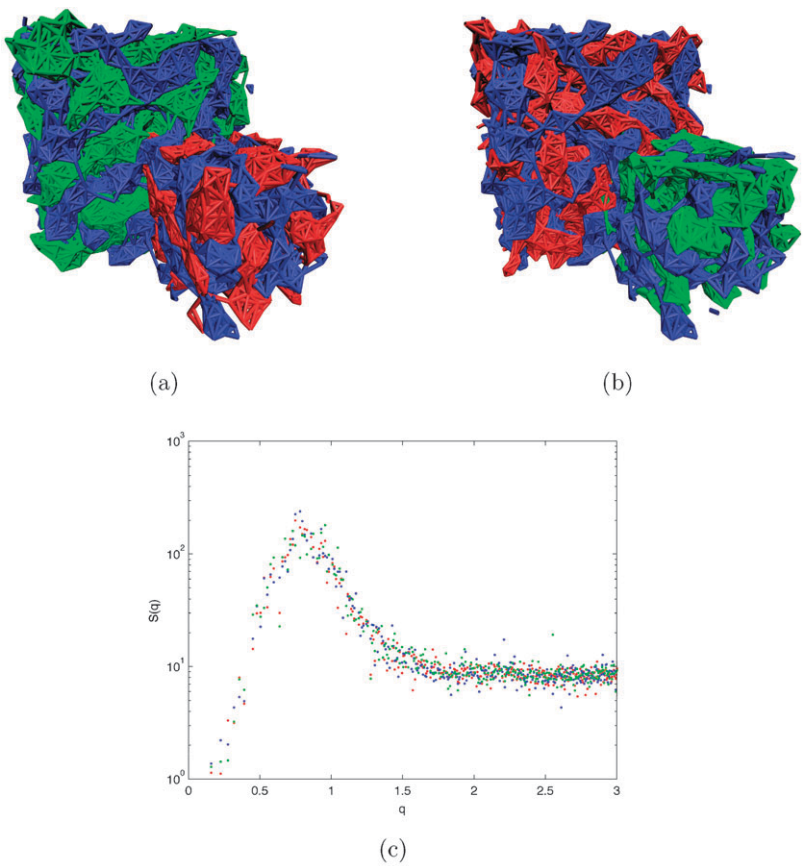

Fig. 4 (a) and (b) Two snapshots of the novel tricontinuous mesophase composed of red, green and blue domains, with various domain pairs highlighted. The images reveal the features of a 'balanced' example, with three geometrically equivalent interwoven 3D domains with long-range translational order. See also movie 1 in the ESI.† (c) Structure factors calculated from the bead centre positions for the differently coloured beads from a single simulation snapshot, illustrating that the three phases are equivalent. Simulation details: 3000 molecules, $L = 39.4\sigma$, $d_0 = 1\sigma$, $\phi = 13$, occupied volume fraction = 0.56, $k_BT = 1.5\varepsilon$, $w_c = 1.6\sigma$.

compared with balanced cases (15–20% in the extreme cases presented below). Volume changes of arms are achieved mainly by swelling induced by increased bead diameters. This is in contrast to the simulations by Dotera and coworkers[16] where relative volume fractions between arms were obtained exclusively by altering the arm lengths.

We discuss here two unbalanced situations. The first contains a single arm that is larger than the other two; the second situation is the converse, where one arm is smaller than the other two. The relevant bead diameters are [1, 0.7, 0.7] in the first case, and [1, 1, 0.6] in the second case, where diameters are ordered as red, blue and green respectively. The results presented below are typical also for a range of relative volumes, from the volume differences in our pair of scenarios, towards more balanced cases (at least for the ranges [1.0, 0.7–0.8, 0.7–0.8] and [1.0, 1.0, 0.6–0.8] in the two scenarios). We focus here on the most asymmetric cases analysed in detail, since these offer a clearer picture of the morphologies.

The first scenario listed above corresponds to a situation where the volume fraction of the red phase is similar to the volume fraction of the blue and green phases combined. The simulation result is shown in Fig. 5. As illustrated in Fig. 5(a) the red majority phase segregates into a sponge-like three-dimensional domain while the two minority components segregate into convex, compact domains (Fig. 5(b)). As shown in Fig. 5(c) (and movie 2 in the ESI†) each compact green domain has four neighbouring blue domains and *vice versa*, arranged such that the globules are centred on nodes of the tetrahedral diamond net. Merging the blue and green domains results in a second three-dimensional sponge-like domain, complementary to the red majority domain. Thus, the overall structure is related to a double diamond network with one of the diamond networks constructed of alternating blue/green domains'. This organisation is illustrated further in Fig. 6.

In contrast to the balanced case analysed above, this first unbalanced pattern necessarily contains triple lines with net curvature. Indeed, these lines form closed loops, lying on the boundaries of the disc-like walls separating adjacent blue and green globular domains. In addition, the triple lines also

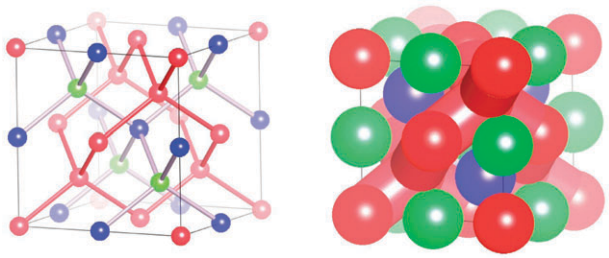

Fig. 6 (a) New domain pattern (with space group symmetry $F\bar{4}3m$) found in simulations of three-arm star-polyphiles with unbalanced arms: the bulkier arm (red) forms a single three-dimensional network pattern whose channels lie along edges of the tetrahedral diamond net. The other two smaller arms form convex globular domains, centred at vertices of a second interwoven 'striped' diamond net, whose vertices are alternately coloured green and blue. (b) A second view, corresponding more nearly to the space-filling domains of the true polyphile mesophase.

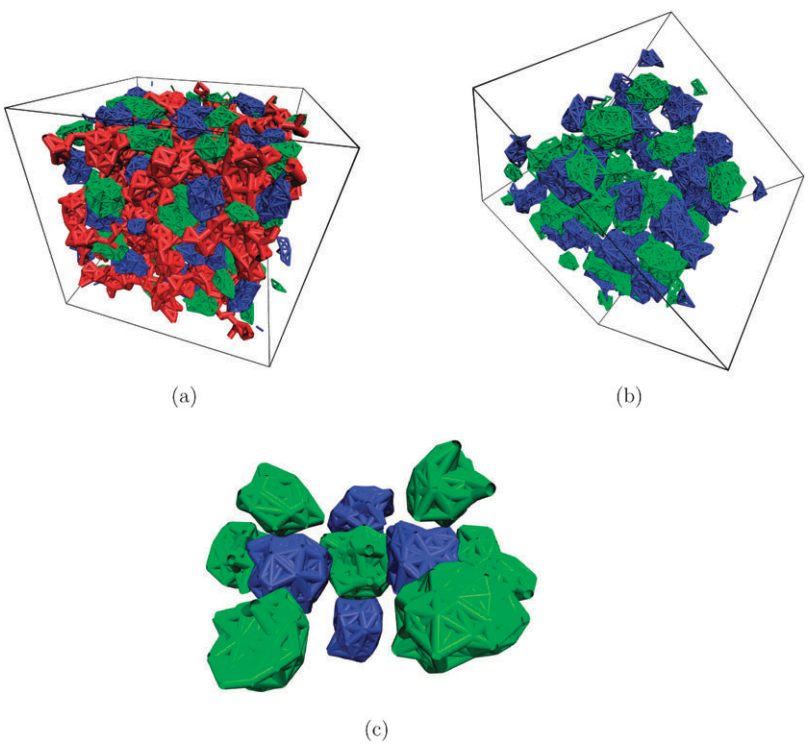

Fig. 5 Simulation with bead diameters [1.0, 0.7, 0.7]. (a) All three domains, showing the sponge-like topology of the red domain. (b) Blue and green globular domains. (c) Close-up of blue and green globular domains showing the four neighbouring green/blue globules coordinating each blue/green globule in a quasi-tetrahedral configuration. See also movie 2 in the ESI†. Simulation details: 1000 molecules, $L = 20\sigma$, $d_0 = d_1 = 1\sigma$, $d_2 = d_3 = 0.7\sigma$, occupied volume fraction = 0.4, $k_BT = 1.5\varepsilon$, $w_c = 1.6\sigma$.

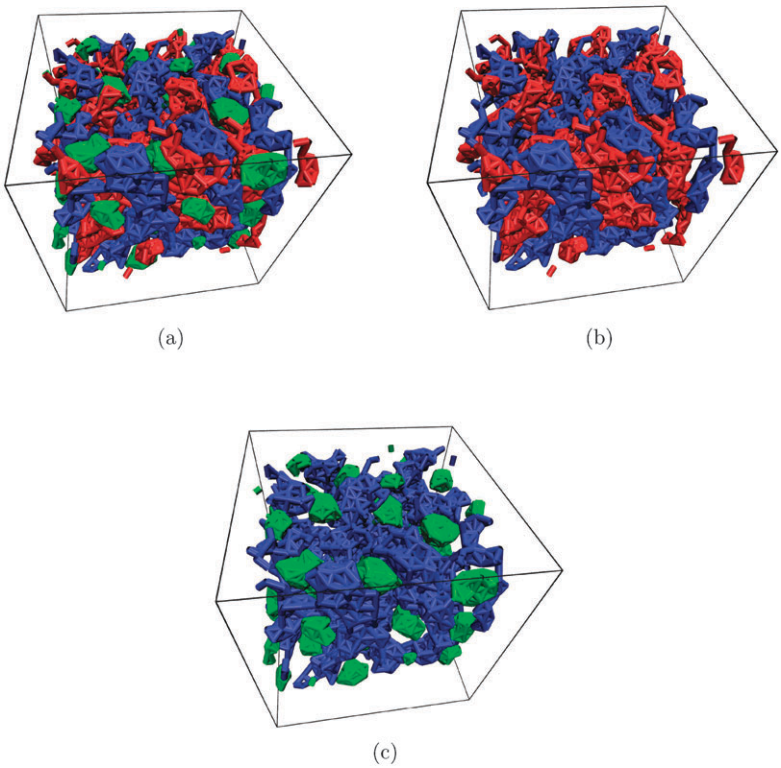

Fig. 7 Simulation with bead radii [1.0, 1.0, 0.6] for the red, blue and green arms respectively. (a) All 3 domains. (b) The pair of bulkier domains (red and blue), showing interwoven sponge-like patterns. (c) The blue majority domain together with the green minority component, that forms isolated globules. Simulation details: 1000 molecules, $L = 22\sigma$, $d_0 = d_1 = d_2 = 1\sigma$, $d_3 = 0.6\sigma$, occupied volume fraction = 0.38, $k_{\mathrm{B}}T = 1.5\varepsilon$, $w_c = 1.6\sigma$.

appear to contain some torsion, since the normal vectors to the domain walls vary around each loop. Therefore, this unbalanced example leads to triple lines that are both curved and twisted.

Fig. 7 shows the pattern that emerges from the simulations by imposing an unbalanced 3-arm star architecture, corresponding to that of the second situation described above. As with the tricontinuous pattern, we have not yet identified the geometric details of the structure. However, the topology of the pattern is to our knowledge novel: here the domains containing the smallest moiety of the polyphile molecules are discrete convex globular domains, as in the previous unbalanced example, discussed immediately above. In contrast to that case, here the two larger moieties each form interwoven three-periodic sponge-like domains (see also movie 3 in the ESI†). In addition, the pattern contains triple lines that are both curved and twisted, as in the previous case.

IV. Conclusions

We have simulated the self-assembly of a novel class of self-assembled molecules, with particular focus on formation of liquid crystalline mesophases. Coarse-grained bead simulations of these three-arm *ABC* star-architecture polyphiles have uncovered a richness of liquid crystalline mesostructures that can be related to the better-known bicontinuous mesophases of lyotropic amphiphilic systems. For convenience, the modelling has effectively imposed equal surface tensions between all three (*AB*, *BC* and *CA*) interfaces. The simulations form 3D self-assemblies whose structural variations appear to follow the variations that are expected assuming a simple steric molecular packing model as a function of star polyphile splay and relative volumes of each arm in the polyphile, where the former feature induces torsion of the interfaces along the triple lines and latter curvature of the triple lines.

We have detected three distinct mesostructures, characterised by the topology of the micro-domains that result from self-assembly. A tricontinuous pattern, containing three interwoven 3-periodic sponge-like domains is found in a range of 'balanced' three-arm star polyphiles, whose arms are of equal volume. The triple lines in this pattern exhibit torsion, to accommodate the splay, but no curvature. In contrast, unbalanced splayed molecules reveal complex mesostructures, with curved and twisted triple lines. One example is a 'striped' bicontinuous pattern, with the most voluminous moiety forming a 3D sponge-like domain, interwoven by a second 3D sponge like domain, that consists of alternating globules of the two less voluminous moieties. This example is closely related to the double-diamond bicontinuous mesostructure based on the D-surface, and is cubic (with space group $F\bar{4}3m$). A distinct unbalanced molecule gives a pattern containing a pair of interwoven 3D sponge-like domains of the two more voluminous fractions of the star polyphile, while the third component forms a 3D lattice of isolated globules.

Evidently, these three- (or more) arm polyphilic systems offer an interesting extension to (two-arm) amphiphilic

self-assemblies. Indeed, the simulations reported here suggest a wider range of mesostructures than has been found to date in amphiphilic systems. We are currently exploring a number of polyphile systems experimentally, encouraged by these simulations. Preliminary results suggest that liquid crystals form readily in these systems, as predicted by the simulations reported here.

Acknowledgements

We gratefully acknowledge the extensive help of Ira R. Cooke in modifying mbtools for our purposes and Markus Deserno for general discussions.

References

1 J. N. Israelachvili, D. J. Mitchell and B. W. Ninham, *J. Chem. Soc., Faraday Trans. 2*, 1976, **72**, 1525–1566.
2 S. Hyde, S. Andersson, Z. Blum, S. Lidin, K. Larsson, T. Landh and B. Ninham, *The Language of Shape*, Elsevier Science B.V., Amsterdam, 1997.
3 S. Sioula, N. Hadjichristidis and E. Thomas, *Macromolecules*, 1998, **31**(23), 8429–8432.
4 S. Sioula, N. Hadjichristidis and E. Thomas, *Macromolecules*, 1998, **31**(16), 5272–5277.
5 A. Zioga, S. Sioula and N. Hadjichristidis, *Macromol. Symp.*, 2000, **157**, 239–249.
6 K. Yamauchi, S. Akasaka, H. Hasegawa, H. Iatrou and N. Hadjichristidis, *Macromolecules*, 2005, **38**(19), 8022–8027.
7 A. Takano, W. Kawashima, S. Wada, K. Hayashida, S. Sato, S. Kawahara, Y. Isono, M. Makihara, N. Tanaka, D. Kawaguchi and Y. Matsushita, *J. Polym. Sci., Part B*, 2007, **45**(16), 2277–2283.
8 A. Takano, S. Wada, S. Sato, T. Araki, K. Hirahara, T. Kazama, S. Kawahara, Y. Isono, A. Ohno, N. Tanaka and Y. Matsushita, *Macromolecules*, 2004, **37**(26), 9941–9946.
9 K. Hayashida, W. Kawashima, A. Takano, Y. Shinohara, Y. Amemiya, Y. Nozue and Y. Matsushita, *Macromolecules*, 2006, **39**(14), 4869–4872.
10 K. Yamauchi, K. Takahashi, H. Hasegawa, H. Iatrou, N. Hadjichristidis, T. Kaneko, Y. Nishikawa, H. Jinnai, T. Matsui, H. Nishioka, M. Shimizu and H. Fukukawa, *Macromolecules*, 2003, **36**(19), 6962–6966.
11 K. Hayashida, A. Takano, S. Arai, Y. Shinohara, Y. Amemiya and Y. Matsushita, *Macromolecules*, 2006, **39**(26), 9402–9408.
12 K. Hayashida, N. Saito, S. Arai, A. Takano, N. Tanaka and Y. Matsushita, *Macromolecules*, 2007, **40**(10), 3695–3699.
13 P. Tang, F. Qiu, H. Zhang and Y. Yang, *J. Phys. Chem. B*, 2004, **108**(24), 8434–8438.
14 A. Takano, W. Kawashima, A. Noro, Y. Isono, N. Tanaka, T. Dotera and Y. Matsushita, *J. Polym. Sci., Part B*, 2005, **43**(18), 2427–2432.
15 T. Dotera and A. Hatano, *J. Chem. Phys.*, 1996, **105**, 8413.
16 T. Gemma, A. Hatano and T. Dotera, *Macromolecules*, 2002, **35**, 3225–3227.
17 Y. Bohbot-Raviv and Z.-G. Wang, *Phys. Rev. Lett.*, 2000, **85**, 3428–3431.
18 T. Dotera and T. Gemma, *Philos. Mag.*, 2006, **86**, 1085–109.
19 C.-I. Huang, H.-K. Fang and C.-H. Lin, *Phys. Rev. E*, 2008, **77**, 031804.
20 I. R. Cooke, K. Kremer and M. Deserno, *Phys. Rev. E*, 2005, **72**(1), 011506.
21 I. R. Cooke and M. Deserno, *J. Chem. Phys.*, 2005, **123**(22), 224710.
22 B. J. Reynwar, G. Illya, V. A. Harmandaris, M. M. Muller, K. Kremer and M. Deserno, *Nature*, 2007, **447**(7143), 461–464.
23 G. Illya and M. Deserno, *Biophys. J.*, 2008, **95**, 4163–4173.
24 I. R. Cooke and M. Deserno, *Biophys. J.*, 2006, **91**(2), 487–495.
25 H. J. Limbach, A. Arnold, B. A. Mann and C. Holm, *Comp. Phys. Comm.*, 2006, **174**(9), 704–727.
26 W. Humphrey, A. Dalke and K. Schulten, *J. Mol. Graphics*, 1996, **14**, 33–38.

